Respiratory bioaccessibility and solid phase partitioning of potentially harmful elements in urban environmental matrices

Alexys Giorgia Friol Boim [a, 1, *]

Carla Patinha [b]

Joanna Wragg [c]

Mark Cave [c]

Luís Reynaldo Ferracciú Alleoni [a]

[a] Department of Soil Science, Luiz de Queiroz College of Agriculture (ESALQ), University of São Paulo (USP), 13418-900, Piracicaba, São Paulo, Brazil.

[b] GEOBIOTEC, Geosciences Department, Aveiro University, Campus de Santiago, 3810-193 Aveiro, Portugal.

[c] British Geological Survey, Environmental Science Centre, Nicker Hill, Keyworth, Nottingham NG12 5GG, UK.

* Corresponding author at: Department of Soil Science, University of São Paulo (ESALQ/USP), Av. Pádua Dias, 11, 13418-900, Piracicaba/SP, Brazil. Tel.: +55 19 3417 2155. E-mail address: agfboim@usp.br (A. G. F. Boim).

[1] Current Address: Department of Oceanography and Ecology, Federal University of Espírito Santo, Vitória, Espírito Santo 29075-910, Brazil.

19 **Respiratory bioaccessibility and solid phase partitioning of potentially harmful elements in urban**
20 **environmental matrices**
21
22 **Abstract**
23
24 Studies regarding the role of geochemical processes in urban environmental matrices (UEM) and their influence
25 on respiratory bioaccessibility in humans are scarce in humid tropical regions, especially in Brazil. Contaminated
26 UEM are potentially hazardous to humans if particles < 10 μm in diameter are inhaled and reach the
27 tracheobronchial region. In this study, we evaluated samples collected in Brazilian UEM with a large
28 environmental liability left by former mining industries and in a city with strong industrial expansion. UEM
29 samples were classified into soil, sediment and mine tailings according to the characteristics of the collection sites.
30 The respiratory bioaccessibility of potentially harmful elements (PHE) was evaluated using artificial lysosomal
31 fluid (ALF, pH 4.5), and the BCR-sequential extraction was performed to evaluate how the respiratory
32 bioaccessibility of the PHE was related to the solid phase partitioning. The bioaccessible fraction (BAF) ranged
33 from 54 - 98% for Cd; 21 - 89% for Cu; 46 - 140% for Pb, 35 - 88% for Mn and; 41 - 84% for Zn. The average
34 BAF of the elements decreased in the following order: Soil: Cd> Pb> Mn> Zn> Cu; Tailing: Pb> Cd> Zn> Mn>
35 Cu; and Sediments: Pb> Mn> Cd> Zn> Cu. BCR-fractions were useful to predict the PHE bioaccessibility (R^2 =
36 0.79 – 0.98), thus suggesting that particle geochemistry and mineralogy can influence PHE behaviour in the
37 pulmonary fluid. Therefore, this approach provides a combination of quantitative and qualitative data, which
38 allows us to carry out a more realistic assessment of the current situation of the potentially contaminated site and
39 possible alternatives for decision-making by the stakeholders.
40
41 **Keywords:** Artificial lysosomal fluids; human inhalation exposure; < 10 μm particulate matter; mineralogy;
42 sequential extraction

Funding sources that supported the work

This study was supported by the São Paulo Research Foundation (FAPESP) [grants # 15/19332-9 and # 15/24483-9]; by the Brazilian National Council for Scientific and Technological Development (CNPq) [grant # 404164/2016].

Highlights

- Artificial lysosomal fluid - ALF can estimate the respiratory bioaccessibility of PHE
- The solid phase distribution provided insights into behaviour of PHE in ALF
- The bioaccessibility varied with the geochemical and mineralogical characteristics
- *In vitro* methods should become part of HHRA procedures

52 **Graphical abstract**

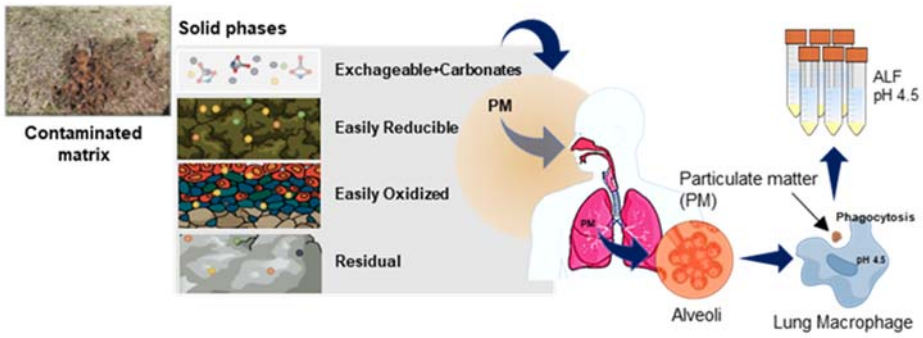

1. Introduction

In the urban environment, potentially harmful elements (PHE) have several sources, such as soils, household dust, vehicular traffic and industrial activity. Urban soils can be a sink of a substantial amount of waste products, including industrial and mining waste and particulate matter emitted by motor vehicles or industrial chimneys whose contaminated particles can be deposited onto the superficial layers of urban soils. Such particulate matter (PM), as fine fraction of soil or dust particles, can subsequently be carried by the wind and reach human respiratory airways.

In the context of human health risk assessment (HHRA), exposure routes are the paths on which contaminants can establish contact with the organism, such as ingestion, dermal contact or absorption and inhalation (USEPA, 1989). Besides, the risk estimate should be determined for each PHE identified at the investigated area, considering the duration of the exposure and the dose-response, that is, the probability that a PHE has to produce adverse effects on the receptors (Jaishankar et al., 2014; Öberg and Bergbäck, 2005).

The risk associated with human exposure to PM can be based on the assumption that inhalation will be the main route reached (Tong et al., 2019; Zhang et al., 2014) either during indoor or outdoor activities. PM is classified into two categories, PM_{10} = aerodynamic diameters <10 μm and $PM_{2.5}$ = aerodynamic diameters < 2.5 μm (USEPA, 2016). According to Kastury et al. (2017), PM10 has a higher risk via inhalation as it can reach the tracheobronchial and alveolar region.

PM_{10} and $PM_{2.5}$ can be suspended in the air for long periods of time, e.g. the PM_{10} can be suspended for a few hours, while $PM_{2.5}$ can remain suspended in the atmosphere for several days to weeks (Leelasakultum and Kim Oanh, 2017) and when inhaled are deposited onto the surfaces of the respiratory system. The inhalation of PM may pose human health in risk by causing various respiratory diseases, such as irritation of the airways, allergic, asthma or others inflammatory reactions and fibrosis (Habybabady et al., 2018; Tong et al., 2019). PM not removed from the body by muco-ciliary clearance, that is, the insoluble particle can be swallowed toward the gastrointestinal tract, may reach the respiratory system becoming susceptible to solubilization by lung fluids (Guney et al., 2016). Thus, PHE exposure risk via inhalation is related not only to the particle size, but also to the type of solid fraction particle that can be easily solubilized in this environment.

The inhaled PM can be transported and trapped in the tracheobronchial system, and PHE bound to the PM can be solubilized by the epithelial lining fluids or extracellular environment. The PHE may be subjected to absorption, and/or diffused within the pulmonary system, even may bind to proteins and some cellular structures reaching the circulatory system (Lehnert, 1990; Oberdörster et al., 2005). When a particle is not solubilized by the

epithelial lining fluid, it can be phagocytized by alveolar macrophage (intracellular environment). The presence of enzymes, oxygen radicals, chelating agents and low pH promotes the dissolution of a variety of substances (Kreyling, 1992). In contrast, Galle et al. (1992)demonstrated that the opposite also might occur in the alveolar region, since alveolar macrophages are able to concentrate and precipitate various elements inhaled, preventing the diffusion of toxic substances into the bloodstream.

The respiratory bioavailability of PHE or organic substances has been estimated using *in vivo* tests with animal models, such as rodents (Moreda-Piñeiro et al., 2011), but these models are generally difficult to reproduce, expensive, time-consuming and have ethical constraints. The *in vitro* methods of respiratory bioaccessibility has been used as a surrogate for *in vitro* tests. The application of lung fluids that simulate the solubilization of the studied material (i.e., PM, dusts) in the respiratory tract and, subsequently, the elemental composition of the leachate were evaluated by Huang et al., 2014; Julien et al., 2011 and Niu et al., 2010.

Respiratory bioavailability is the PHE concentration that crosses the barrier between air and blood reaching the circulatory system, while respiratory bioaccessibility is the PHE concentration solubilized on the lung fluids that lining the respiratory system, but it does not necessarily cross the air-blood barrier, that is, it is considered potentially available to humans (Kastury et al., 2017). Molina et al. (2013) evaluated the bioaccessibility of Zn by simulating synthetic lung fluid, mimicking the phagolysosomal fluid at pH 4.5 (intracellular environment) and the bioavailability assisted by intranasal administration of Zn (from Zn mine waste and minerals) in rodents and observed a positive relationship between the *in vivo* and *in vitro* tests ($R^2 = 0.86$). However, there is no standardised procedure (Calas et al., 2017; Kastury et al., 2017; Pelfrêne et al., 2017) in which *in vitro* methods can be compared with *in vivo* studies.

These tests have been used to evaluate respiratory bioaccessibility in environmental matrices: Huang et al. (2014), Julien et al. (2011) and Niu et al. (2010) evaluated the respiratory bioaccessibility of PHE from atmospheric particles (i.e. household air-conditioning filter dust, PM2.5, airborne particulate matter). Similarly, Boisa et al. (2014), Drysdale et al. (2012), Guney et al. (2017), Pelfrêne et al. (2017) and Wragg and Klinck (2007) have used these tests to measure the respiratory bioaccessibility of PHE from soil; Colombo et al. (2008) and Witt III et al. (2014) have assessed road dust; oxide nanoparticles have been investigated by Cruz et al. (2015) and Zhong et al. (2017); and pharmaceutical materials have been looked at by Marques et al. (2011) and Tronde (2002).

Simulated lung fluids (SLF), as Gamble's solution, are widely used to simulate the extracellular lung fluids and estimate the concentration of PHE potentially available for absorption via respiratory tract (Drysdale, 2012; Wragg and Klinck, 2007). Another SLF widely used is the artificial lysosomal fluid (ALF), which simulates

a more acidic environment (pH value of 4.5, against 7.3 for Gamble solution) and mimics the intracellular conditions in the lungs, i.e., the particle comes into contact with the lung fluids after being phagocytosed by alveolar and interstitial macrophages (Calas et al., 2017; Colombo et al., 2008). The presence of complexing ligands (organic acids) and the low pH in the intracellular environment may release PHE adsorbed to oxides, since the complexation of polyvalent cations with chelating agents (e.g. citrate acid) can increase the mobilisation of PHE in the lung (Calas et al., 2017; Wiseman, 2015).

The SLF may alter the speciation of PHE in the solid fraction of the inhaled matrix. However, the properties of each type of matrix can reflect on the behaviour of a PHE dissolved by the fluid lining in the respiratory system, which led us to hypothesize that the PHE associated with more labile solid phases (soluble and exchangeable) in the soil and those phases associated with Fe oxides or/and organic matter in fine soil particle (< 10 μm) can be released into the pulmonary tract. This highlights the importance of characterizing the mineralogy and the solid phase partitioning of environmental matrices in conjunction with *in vitro* bioaccessibility tests to have a set of quantitative and qualitative data and information to obtain more realistic estimates of risk human health.

Mine tailings, generally, have high concentrations of PHE associated with solid particulate matter (i.e. PM10 or PM2.5) and can be easily carried by winds or water runoff. A large volume of tailing is generated during the ore beneficiation process and, most of the time, they are arranged in places with little or no monitoring plan and inspection. Historical mining disasters in Brazil and worldwide still pose a threat to human and environmental health because of the legacy of associated contaminants. In this study, we collected UEM samples from a Brazilian city with the worst social-environmental disaster associated with mine tailings: the Santo Amaro city, located in the State of Bahia, northeast region of Brazil. In the 1980s, a lead (Pb) smelter operated in the city, producing approximately 900,000 tons of metallic Pb from galena (PbS) concentrate, yielding about 490,000 tonnes of Pb tailings (CETEM, 2012). The tailings material was donated to the locals and to city hall to pave access roads, backyards, streets and public places in the city. The material was also deposited on the soil (open air) and contaminated groundwater and the Subaé River (de Andrade Lima and Bernardez, 2011; de Andrade and Moraes, 2013). The magnitude of the result in complex effects on the environment, and the society often does not have adequate answers about how much and how long they directly affect the health of the exposed population. Therefore, studies of urban soils in areas that were previously associated to some industrial activity are necessary. Principally, for those sites that have been abandoned (commonly called, *brownfields*), and are contaminated or

with suspected of contamination, because humans can be exposed directly to the soil surface and windblown materials or dust.

In vitro bioaccessibility methods give an estimate of hazard exposure and provide a line of evidence for HHRA. Such information can inform adequate management of contaminated land relative to the risk of population exposure to health hazards (Cave, 2012). This study presents the results of *in vitro* respiratory bioaccessibility testing of PHE (Cd, Cu, Pb, Mn and Zn) from a set of soil, tailings and sediment samples collected in three Brazilian cities. These samples had contrasting chemical, physical and mineralogical attributes and a wide range of total PHE concentrations. The influence of solid-phase partitioning on the PHE bioaccessibility was investigated by coupling *in vitro* and sequential extraction methods. This is the first study involving respiratory bioaccessibility carried out on particulates from the Brazilian urban environment. Thus, it is expected to serve as a reference or recommendation for the use of *in vitro* methods as part of HHRA procedures and could help in the development of public policies by environmental agencies and other stakeholders to evaluate potentially contaminated areas.

2. Material and Methods

2.1 Collection and sampling areas

To understand the inhalation bioaccessibility and solid phase partitioning of bioaccessible PHE within environmental matrices (soils, sediments and mining tailings) samples of urban environmental matrices were collected in three Brazilian cities. The selection of samples was taken at random to obtain a set of heterogeneous samples with contrasting physical, chemical and mineralogical characteristics.

The samples were collected from the cities of Piracicaba (n = 3), the eastern region of the state of São Paulo (SP), Brazil; Apiaí (n = 5), Upper Ribeira Valley (SP); and Santo Amaro (n = 9), in the concave region (Recôncavo Baiano), state of Bahia (BA), Brazil (Table 1 and Figures S1, S2 and S3 (Supplementary Material)). In Piracicaba, soil samples were collected from Mario Telles Square, José Bonifácio Square and at the athletics track of the Luiz de Queiroz College of Agriculture, University of São Paulo, near Independência Avenue, one of the busiest roads in the city (Table 1, Fig. S1). All are recreational sites in residential areas frequented by children but are also characterized by high traffic density.

The samples from Apiaí were collected from the Centre for Integrated and Multidisciplinary Studies of Apiaí (CIEM), a unit of the Mineral Resources Research Company (CPRM) of Geological Survey of Brazil, located in the Upper Ribeira Valley Region (Table 1, Fig. S2). A Pb and silver (Ag) foundry and an old slag deposit operated in this area (Calabouço Mill) from 1940 to 1956. The main environmental issues in this area are mineral

dust, metallic waste and Pb slag deposits (Martins and Figueiredo, 2014). The samples were collected from five sites: four in the CIEM area containing soil associated with Pb tailings (Fig. S2) and were classified as mining tailing contaminated; other one was collected in the native forest near the unit and was classified as soil. The sampling locations were selected based on a metal distribution map from a study carried out by Martins and Figueiredo (2014).

In Santo Amaro, the identification of suitable sample collection sites was based on the "Map of soil contamination by chemical elements in Santo Amaro da Purificação" (Carvalho et al., 2010). Samples were collected from within the city perimeter, including the former lead smelter, which ceased activity in 1993 (CETEM, 2012). People who worked or lived in Santo Amaro during the operational period of the company indicated where the slag was deposited. A total of nine samples were collected: one tailing (collected in the deactivated plant area), four soils (samples collected in residential areas, mainly frequented by children) and four sediments (two samples collected on the banks of the Subaé river and the other two samples collected into a street gutter and in an unpaved road close to the plant area) (Table 1, Fig. S3). Samples classified as sediments commonly had high sand contents (2SA and 3SA) and contained some materials possibly derived from the old Pb metallurgical (7SA and 8SA) operations.

Each sample was composed of five subsamples collected from the 0-5 cm layer (across an area of approximately 4 m^2) using a stainless-steel shovel and thoroughly mixed to obtain approximately 5 kg of soil. The samples were then placed in plastic bags and transported to the laboratory. The depth of 0-5 cm was chosen because it is assumed that this is the soil layer that can be carried by the wind and thus can cause risk to human through inhalation/ingestion pathways (Drysdale et al., 2012). The samples were air dried, sieved to < 2 mm, coned and quartered to provide a representative sample for further chemical, physical and mineralogical analyses. Each sample was stored in plastic pots and classified according to the type of matrices: soil, sediment and tailings. This classification was necessary to allow the evaluation of the effect of ALF solution on different matrices.

195 **Table 1.** Identification of urban environmental matrices, coordinates and sites characteristics of the local collection
196 of soil, sediments and tailing matrices

#ID	Classification	City	Coordinate		Site
35PC	Soil	Piracicaba	22°42.054'S	47°40.072'W	Mario Telles Square and Playground
47PC	Soil	Piracicaba	22°43'27"S	47°38'52.94"W	José Bonifácio Downtown Square
58PC	Soil	Piracicaba	22°42.850'S	47°37.975'W	Athletics track of the Luiz de Queiroz College of Agriculture campus
3SA	Soil	Santo Amaro	12°33.111'S	38°42.514'W	Saudade Cemetery Garden
5SA	Soil	Santo Amaro	12°33.287'S	38°41.675'W	Neighbourhood Derba, residential area
6SA	Soil	Santo Amaro	12°32.406'S	38°43.637'W	Soccer field for children near the old company facilities
9SA	Soil	Santo Amaro	12°33.651'S	38°42.073'W	Garden of Municipal School Maria dos Anjos Salles Brasil
5AP	Soil	Apiaí	24°32.443'S	48°49.851'W	Native forest, next to the old company facilities
2SA	Sediment	Santo Amaro	12°32.804'S	38°42.491'W	Subaé riverbank, next to Pedro Lago School
4SA	Sediment	Santo Amaro	12°33.019'S	38°42.385'W	Subaé riverbank, near the Forum
7SA	Sediment	Santo Amaro	12°32.427'S	38°43.632'W	Unpaved road connecting Rui Barbosa Avenue and the old facilities
8SA	Sediment	Santo Amaro	12°32.415'S	38°43.602'W	Street gutter of Rui Barbosa Avenue
1AP	Tailing	Apiaí	24°32.315'S	48°49.991'W	Soil with slag from the landfill at old company facilities
2AP	Tailing	Apiaí	24°32.323'S	48°49.909'W	Soil with slag from the landfill at old company facilities

3AP	Tailing	Apiaí	24°32.356'S	48°49.955'W	Soil with slag from the landfill at old company facilities
4AP	Tailing	Apiaí	24°32.349'S	48°49.899'W	Soil with slag from the landfill at old company facilities
1SA	Tailing	Santo Amaro	12°32.371'S	38°43.855'W	Soil with slag from the landfill at old company facilities

197

198 **2.2 Preparation of the samples for the *in vitro* test**

199 The main interest was focused on particles with aerodynamic diameter of < 10 µm because these particles
200 affect the tracheobronchial system and can reach the alveolar region (Boisa et al., 2014; Guney et al., 2017).
201 Samples for respiratory bioaccessibility testing were prepared by mechanically shaking the 2 mm size fraction
202 through a series of 1 mm, 500 µm, 250 µm, 125 µm and 63 µm (18, 35, 60, 120 and 230 Mesh) sieves for 30 min.
203 The resulting material was retained in a collector and stored in plastic pots prior to further separation to obtain the
204 10 µm fraction. All materials used were plastic, except for sieves, which were made of stainless steel, to avoid
205 contamination.

206 The separation method was adapted from Lijung et al. (2011, 2008). Approximately 40 g of the < 63 µm
207 sub-sample was transferred to a 600 mL beaker containing 500 mL of ultrapure water (18 ΩM cm^{-1}). The
208 suspension was shaken by hand, followed by ultrasonic dispersion for 5 min (three times), allowed to stand for 10
209 min and filtered using a 10 µm aperture nylon filter with the aid of a vacuum pump. The supernatant was transferred
210 to a beaker and dried at 60 °C for three days. After drying, samples were gently disaggregated using an agate pestle
211 and mortar, stored in plastic pots previously washed with 10% HCl and rinsed with ultrapure water.

212 The amount of material filtered at 10 µm varied between the samples ranged from 1 to 12 g (data not
213 shown). This fraction was nominated as "fine fraction" or "FF" (diameter < 10 µm) to differentiate it from bulk
214 sample (BS), that is, the sample as a whole (< 2 mm).

215

216 **2.3 Chemical and physical characterization of bulk samples (BS)**

217 The samples were characterized as follows: pH in water (1:2.5, m/v), granulometric fractions by
218 densimeter, both methods described by Donagema et al. (2011); Total carbon (TC) concentration was determined
219 by catalytic combustion oxidation at 900ºC and measured by a non-dispersive infrared sensor (NDIR) in a Total
220 Organic Carbon Analyzer, model TOC-L (Shimadzu), coupled in a sampler for solid samples SSM 5000A,

Shimadzu. The determination of pseudo-total concentration of PHE was carried out in triplicate after acid extraction assisted by a microwave according to method USEPA 3051A (1:3 HCl: HNO_3, v/v) (USEPA, 2007), in both fractions, BS (determined by optical emission spectroscopy with inductively coupled plasma (ICP-OES)) and FF (determined by inductively coupled plasma mass spectrometry (ICP-MS)).

2.4 Determination of respiratory bioaccessibility of PHE in the soil, sediment and tailings matrices

To simulate the intracellular conditions in lung fluids, an ALF solution was prepared as described in Pelfrêne et al. (2017). For this purpose, 0.05g (± 0.0001) of the FF was weighed in 85 mL polycarbonate centrifuge tubes, and 50 mL of the simulated fluid (ratio - 1:1000) were added. This ratio was one of those studied by Pelfrêne et al. (2017), who observed that bioaccessibility does not depend on the soil: solution ratio from 1:1000 to 1:10000.

Samples were shaken at 37 ºC on an end-over-end shaker for 24 h and centrifuged at 4500 × g for 15 min. This extraction time was chosen because Cruz et al. (2015), Pelfrêne et al. (2017) and Guney et al. (2017) have shown that it is enough for maximum dissolution of the soil PHE. The extracts were diluted 1:10 with 2% HNO_3 and transferred to polypropylene tubes and kept under refrigeration until determination in ICP MS. For each element, the bioaccessible fraction (BAF%) for the lung compartment was calculated according to the following equation:

$$BAF\ (\%) = \frac{ALF_{conc}}{FF_{pseudototal}} \times 100$$

where: ALF_{conc} = respiratory bioaccessible PHE concentration extracted by ALF (mg kg^{-1}) and $FF_{pseudototal}$ = PHE pseudo-total concentration of the fraction of < 10µm (FF) (mg kg^{-1})

2.5 Sequential Extraction

The BCR-modified method (Rauret et al., 1999) has been successfully applied in studies with several environmental matrices such as soils, sediments and dust (Kasemodel et al., 2019; Lu and Kang, 2018; Unda-Calvo et al., 2017; Zhao et al., 2018). The sequential extraction was performed according to Rauret et al. (1999) in three steps. For this, 0.5 g of FF sample was weighed, instead of 1 g as described by Rauret et al. (1999), and the solid:volume ratio maintained. This was done because of limitations in the amount of FF samples obtained (Section 2.2). To perform sequential extraction, steps were carried out as follows:

(i) F1: the soluble, exchangeable phase (non-specifically adsorbed species) and carbonate-bounded fraction, extracted with 20 mL of 0.11 mol L^{-1} CH_3COOH and shaken for 16h on an end-over-end shaker at room temperature;

(ii) F2: reducible phase, i.e., bound to the Fe and Mn oxides and oxyhydroxides, extracted with 20 mL of 0.5 mol L^{-1} $NH_2OH.HCl$ and shaken for 16h at room temperature; and

(iii) F3: oxidizable fraction, i.e., bound to organic matter and sulphides, extracted with 5 mL of hydrogen peroxide (300 mg g^{-1}, 8.8 mol L^{-1}) with occasional manual shaking during 1h. The digestion was continued for 1 h at 85 ± 2 ° C in a water bath to allow the sample volume to reduce to <3 ml. This step was repeated twice. Then, 25 mL of 1 mol L^{-1} ammonium acetate (pH 2 adjusted with concentrated HNO_3) was added to the residual material and stirred for 16h at room temperature.

All the supernatants were separated from solid sample by centrifugation for 20 min at 3000 x *g and* preserved under refrigeration at 4ºC prior to analysis. The residual solids were then washed with 10 ml of ultrapure water (18 ΩM cm^{-1}), shaken for 15 min and centrifuged for 20 min at 3000 x *g*. The "washing" supernatants were discarded, taking care not to discard the solid residue.

The residual fraction was calculated according to equation: $F4 = FF_{pseudototal}$ (mg kg^{-1}) - Σ[F1, F2, F3 (mg kg^{-1})] (Abdu et al., 2012; Puga et al., 2016). The residual fraction is associated with the elements strongly adsorbed to the crystalline matrix, mainly by specific adsorption, suggesting predominantly a geogenic origin (Patinha et al., 2015).

2.6 Quality assurance and control

The determination of the PHE concentration was performed by Inductively Coupled Plasma Atomic Emission Spectroscopy (Thermo Scientific iCAP 6300 Duo, ICP OES) for the determination of the pseudo-total concentrations of the PHE of the BS and the PHE concentrations of the fractions of the sequential extraction. Inductively Coupled Plasma Mass Spectrometry (Agilent 7700x, ICP MS) was used to determine the pseudo-total and bioaccessible PHE concentrations, both from the FF samples.

For quality assurance and control, samples of standard reference material (SRM) NIST 2711a (NIST, 2009) were included in the pseudo-total (BS samples) digestion (n = 2) and a SRM BCR 723 (Road Dust) sample was used in the pseudo-total extraction (FF samples) and bioaccessibility procedures (n = 2) (Table S1). Mean recoveries for the selected elements in all SRMs varied from 70 - 126%, and relative standard deviations (RSDs) for all replicates were < 10%. The analytical blanks contained PHE concentrations below the limit of quantification (LQ): 0.005 (Cd, Cu and Mn), 0.01 (Pb), 0.05 (Zn) mg L^{-1} (ICP OES) and 0.003 (Cd and Cu), 0.03 (Pb), 0.1 (Mn), 0.004 (Zn) mg L^{-1} (ICP MS).

All tests were performed with ultrapure water (18.2 MΩ). All plastic and glassware used was washed with Extran® detergent (3%) and rinsed with deionized water followed by soaking in 10% HCl for 24h. Finally, all equipment was rinsed with deionized water followed by ultrapure water and placed in an oven to dry at 45 °C.

2.7 X-ray diffraction

All BS (bulk samples (< 2 mm)) were ground in a tungsten mill and sieved to < 100 μm for the identification of the crystalline materials in the urban matrices.

The clay fraction was analysed after treatment with sodium dithionite-citrate-bicarbonate solution (DCB) to eliminate the crystalline Fe oxides and consequently concentrated the silicates in the sample soils. The clay samples were then treated as follows: (i) magnesium (Mg) saturation and air drying to distinguish between the expansive and non-expansive 2:1 minerals; (ii) Mg saturation and glycerol solvation to differentiate vermiculites from smectites (2:1 minerals); (iii) saturation with potassium (K),air drying and heating to 110, 350 and 550 °C in a muffle to differentiate chlorite from interstratified minerals, 2:1 and 2:2 minerals and for the destruction of 1:1 minerals, such as Kaolinite (Dixon and Weed, 1989).

The mineralogical identification was performed by X-ray diffraction (XRD) using a Philips PW 1877 diffractometer operated at a potential of 40 kV, 40 mA currents, CuKα (k = 1.54186 Å), with a monochromator for the elimination of Kβ radiation, and step increment of one second for each 0.02º (2θ). The samples were deposited on glass slides or a sampler holder and analysed in a scanning range of 3º to 65º (2θ).

2.8 Statistical Analyses

The SPSS Statistics 20 (SPSS Inc.) software was used for descriptive statistics and for parametric and non-parametric tests. The non-parametric tests Kruskal-Wallis and Wilcoxon-Mann-Whitney were chosen rather than ANOVA, because of their better applicability for small samples size (n < 30) with groups of different sizes (Marôco, 2011). As the sample size was < 50 the Spearman correlation was used to evaluate the degree of correlation between the variables. Simple (SLR) and multivariate (MLR) linear regression were used to evaluate the relative impact of PHE pseudo-total concentrations and sequential extraction fractions as predictors of PHE bioaccessibility.

The significance of the regression parameters was verified by the F-test ($p < 0.05$). The assumptions of linear regression were verified by the tests of multicollinearity, homoscedasticity, normality and independent errors (Durbin-Watson test). The MLR model was developed by the *stepwise* selection method. The data were log-

transformed to normalize their distribution. The logarithmic data were again submitted to the analysis of compliance with the assumptions of the MLR to verify whether the transformation was efficient in adapting the variable to the violated assumption.

3. Results and discussion

3.1 Sample characterization

The chemical and physical characteristics determined in the BS (2mm) are summarized in Table 2 and in the whole dataset in the Supplementary Material (Table S2). The pH varied from 4.2 to 7.1, wherein, soils pH had greater variation (4.2 to 7.1) as compared to sediment (6.6 to 7.1) and tailing (5.2 to 6.6) sets. The total carbon (TC) variation was smaller in the sediments (0.5 to 1.3%) compared to the soils (0.8 to 6.3%) and tailings (0.6 to 3.4%). The median content of clay, silt and sand were similar between the three sample types. According to FAO (2014) textural classification the samples were classified as sand, loamy sand, sandy loam, sandy clay loam, clay loam, sandy clay and clay.

The samples showed diverse characteristics as expected, even those samples collected from the same city. Random sites were chosen for sampling, and the collection was carried out in the most superficial soil layer (5 cm), that is usually disturbed by anthropogenic activities. Soils from urban areas may have received various inputs from unknown sources over the years, which may be accumulated in the first centimetres, except for the samples classified as tailings, in which all samples were collected from old landfills slag of the galena beneficiation.

Pseudo-total concentration of PHEs in the BS and FF samples varied greatly (Fig. 1 and Table 2), with the highest concentrations found in the samples collected in the mine tailings areas in the city of Apiaí, with concentrations > 1% for some elements, particularly Pb 8% (BS) and 6% (FF) in sample 1AP (Table S2). The Wilcoxon test showed that the concentrations in BS and FF differed for Cu ($Z = -2.58$; $p = 0.01$) and Cd ($Z = -2.63$ $p = 0.009$), where Cu had a higher median in FF (93.2 mg kg^{-1}) than in BS (69.7 mg kg^{-1}), while Cd had a higher median in BS (14.1 mg kg^{-1}) than in FF (4.6 mg kg^{-1}, Fig. 1, Table 2). Commonly, PHE tend to accumulated in fine fraction probably due to the greater specific surface area that provides higher cation adsorption (Luo et al., 2011), but the opposite was observed for Cd, mainly in the tailing samples (Table S2) in which the concentration and distribution of PHE were not only related to tailings particle size fraction, but probably related to the mineralogical composition as well, as phyllosilicates and Fe oxy-hydroxides (Wei et al., 2015).

Cd had the highest pseudo-total concentrations in the BS in most of samples (Tables 2 and S2). A positive correlation was found between Cd and silt (($r = 0.671$, $p < 0.001$) and between Cd and organic carbon (C-org) (r

340 = 0.486, $p < 0.05$) and a negative correlation between Cd and sand (r = -0.547, $p < 0.05$) in the BS samples (data
341 not shown). This infers that the Cd concentrations could be directly related to silt size (63 to 2 µm). The occurrence
342 of components from organic matter could serve as silt particle coating and generate Cd adsorption sites.
343
344 **Table 2** Chemical and physical characterization, pseudo-total and bioaccessible concentrations of potentially
345 harmful elements (PHE) of samples collected in urban regions in Brazil.

Parameters	Particle size	Minimum	Maximum	Percentiles		
				25th	50th (Median)	75th
Chemical and Physical characterization						
pH	2 mm	4	7	6	7	7
C-total (%)	2 mm	1	6	1	2	3
Sand (%)	2 mm	18	90	33	56	69
Silt (%)	2 mm	4	29	11	18	27
Clay (%)	2 mm	6	55	16	25	40
Pseudo-total concentration						
Cd (mg kg^{-1})	2 mm	<0.1	134.0	3.5	14.1	21.8
Cu (g kg^{-1})	2 mm	<0.1	21.1	<0.1	0.1	0.3
Mn (g kg^{-1})	2 mm	0.1	1.9	0.2	0.4	0.9
Pb (g kg^{-1})	2 mm	<0.1	82.5	0.1	0.7	7.0
Zn (g kg^{-1})	2 mm	<0.1	11.6	0.1	0.5	3.5
Cd (mg kg^{-1})	10 µm	0.2	122.0	0.6	4.6	12.5
Cu (g kg^{-1})	10 µm	0.1	22.5	0.1	0.1	0.4
Mn (g kg^{-1})	10 µm	0.3	1.2	0.5	0.6	0.8
Pb (g kg^{-1})	10 µm	0.1	67.7	0.2	0.4	6.0
Zn (g kg^{-1})	10 µm	0.1	15.7	0.4	0.6	3.5
Bioaccessible concentration						
Cd (mg kg^{-1})	10 µm	0.2	98.5	0.5	4.2	10.7
Cu (g kg^{-1})	10 µm	<0.1	20.0	<0.1	0.1	0.3
Mn (g kg^{-1})	10 µm	0.2	0.9	0.3	0.4	0.6

Pb (g kg^{-1})	10 µm	<0.1	60.7	0.2	0.4	5.4
Zn (g kg^{-1})	10 µm	<0.1	9.9	0.2	0.5	2.7

346

347 For the other elements (Pb, Mn, and Zn) there was no difference ($p > 0.05$), shown by the Wilcoxon test
348 between BS and FF. PHE can be associated with either Fe and Mn oxides or aluminosilicate minerals and
349 incorporated into the structure of minerals present in coarser soil fractions (Batista et al., 2018). Batista et al.
350 (2018) found Pb associated with Fe and Mn, such as plumboferrite [$Pb_2Mn^{2+}_{0.2}Mg_{0.1}Fe^{3+}_{10.6}O_{18.4}$], and primary
351 minerals, such as trioctahedral mica. These authors also found Pb minerals, cerussite ($PbCO_3$), magnetoplumbite
352 [$Pb_{1.1}Fe^{3+}_{7.7}Mn^{3+}_{2.6}Mn^{2+}_{0.6}Ti_{0.6}Al_{0.4}Ca_{0.1}O_{19}$], humboldtine [$Fe^{2+}(C_2O_4)\cdot 2(H_2O)$]) and plumbogummite
353 [$PbAl_3(PO_4)_2(OH)_5\cdot H_2O$] in sand and silt fractions, particle size > 2 µm.

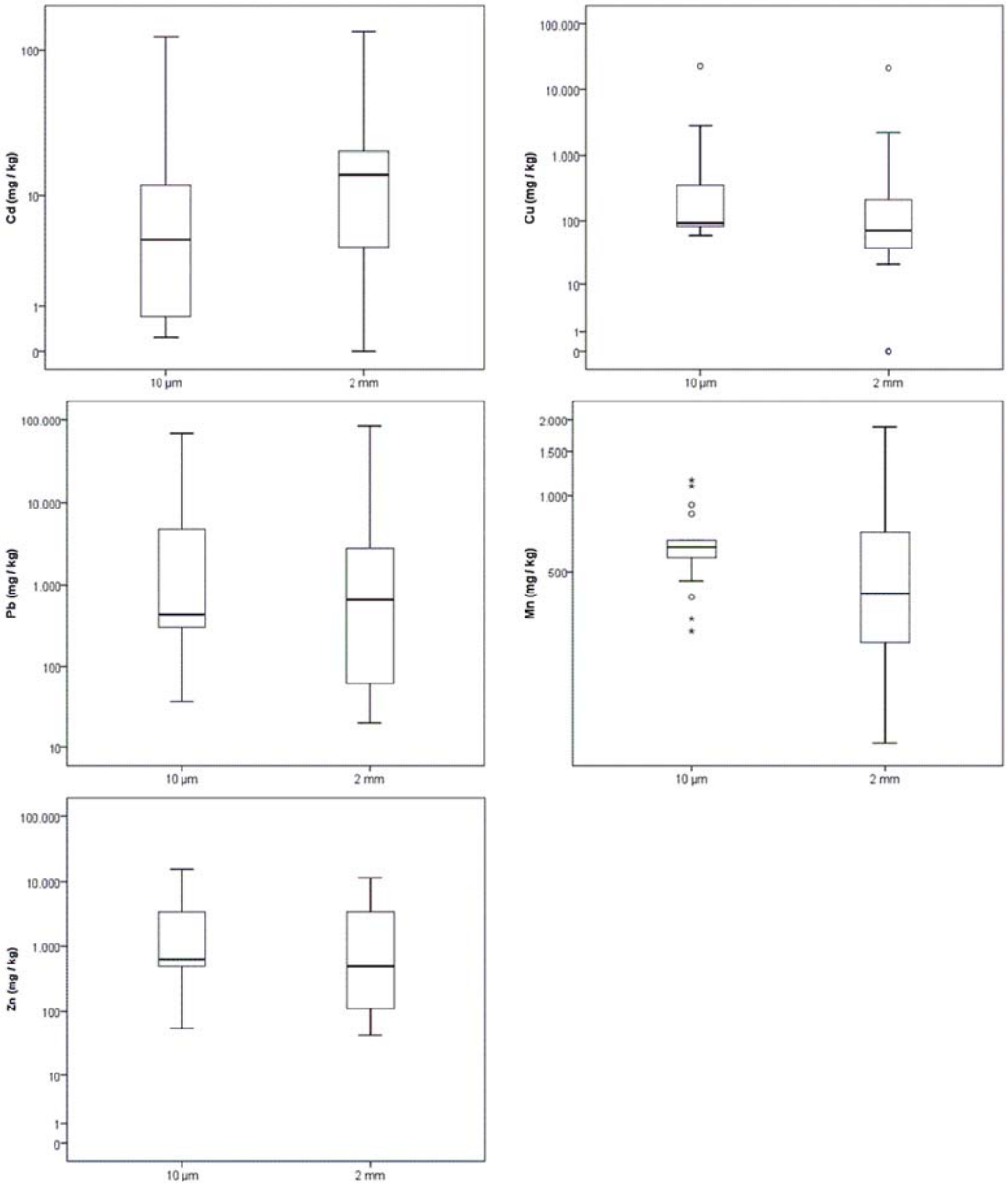

354

355 **Figure 1** Distribution of potentially harmful elements in the bulk sample (2mm) and fine fraction (10μm) of the
356 urban environmental matrices. Data has been log-transformed for better visualization.
357
358 The main minerals identified by XRD in all clay fractions from BS were kaolinite, with illite-
359 montmorillonite, gibbsite and calcite found in smaller amounts (Figure 2). In sample 1AP (tailing), peaks (0.315
360 and 0.307 nm) corresponding to lead oxide (PbO) were observed. XRD analyses were not performed on the FF
361 samples due to small amount of material available. The concentrations of Cu and Zn are relatively high in tailing
362 samples (Table S2); however no crystalline phases associated with these elements were found, but it can be inferred
363 that these elements are in the form of amorphous oxides or insoluble precipitates, probably due to sample pH (5.2
364 to 6.6). Peaks of kaolinite and small amounts of minerals 2:1 and gibbsite were observed in the soil and sediment
365 samples (Figure 2).
366 Although the PHE concentrations in BS and FF were not different ($p > 0.05$) for most elements, the
367 bioaccessibility and fractionation analyses were performed on FF, since this fraction has a greater potential risk to
368 humans, mainly when inhaled (Witt et al., 2014).
369

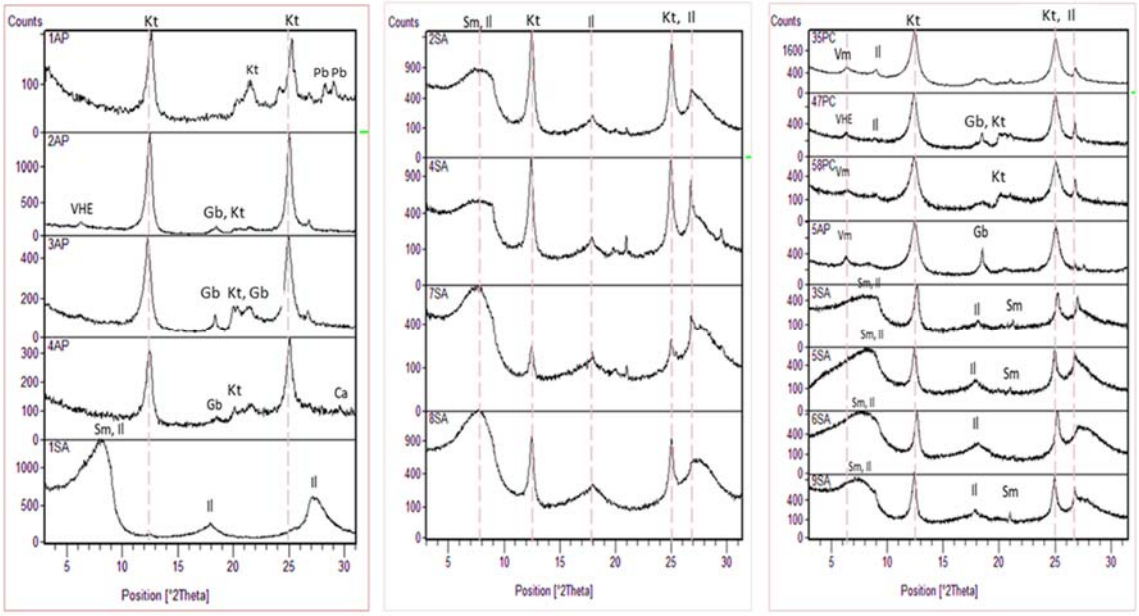

370
371 **Figure 2** X-ray diffraction of urban environmental matrices - Kaolinite (Kt), Gibbsite (Gb), Smectite mineral
372 group (Sm), Illite (Il), Calcite (Ca), Vermiculite (Vm), Hydroxy-interlayered Vermiculite (VHE), Lead oxide (Pb)
373
374 **3.2 Respiratory bioaccessibility of PHE in different environmental matrices**

375 The bioaccessible PHE concentration varied widely among matrices, indicating that they were influenced
376 by the chemistry, physical and mineralogical characteristics, as well as the land uses of the sample matrix (Table
377 1 and S2). The median bioaccessible concentration were 0.5 (Cd); 31 (Cu); 193 (Pb); 325 (Mn) and 239 (Zn) mg
378 kg^{-1} for the soil matrix; 5 (Cd); 49 (Cu); 648 (Pb); 512 (Mn); and 482 (Zn) mg kg^{-1} for the sediment matrix, and
379 11 (Cd); 950 (Cu); 416 (Mn) mg kg^{-1}; and 3 (Zn) and 10 (Pb) g kg^{-1} for the tailing matrix (data not shown).
380 The tailing matrix, as expected, had the highest bioaccessible concentrations of PHE, but some soil (6SA)
381 and sediment (8SA) samples collected in Santo Amaro also had high levels of bioaccessible Cd (20 and 12 mg kg^{-1}),
382 Pb (4,812.1 and 2,014.7 mg kg^{-1}) and Zn (2,516.9 and 1,849.0 mg kg^{-1}) compared to the housing investigation
383 value (IV-H) of regulatory guidance from Brazilian National Environment Council (CONAMA) (Resolution #
384 420, 28/12/2009,(CONAMA, 2012)) established for soils in residential areas (8, 300 and 1000 mg kg^{-1},
385 respectively). The Brazilian intervention values were derived based on generic scenarios (agricultural, housing
386 and industrial) considering characteristics of the physical environment, human behaviour and length of stay in the
387 site. In addition, the methodology includes exposure pathways for each substance present in the soil, such as
388 ingestion and inhalation of soil particles (Dias et al., 2006).
389 According to CONAMA #420/2009, concentrations of PHE in soils above the IV-H may present direct
390 or indirect risks to human health and that the fulfilment of requirement to the contamination control should be
391 made for hazard elimination or reduction. Even though the bioaccessible respiratory concentration was determined
392 in the FF samples, we compared the results with the IV-H established by CONAMA, as there is no protocol in the
393 country that adopts *in vitro* bioaccessibility methods as a requirement for an HHRA.
394 Samples 6SA and 8SA were collected from a soccer field and the sidewalk located on an avenue near an
395 old of Pb metallurgical facility. The presence of these elements at these sites is probably associated with a flood
396 that occurred in 2015, prior to soil collection, when several particulates and coarse materials, derived from the
397 plant, were transported to the sites. The sample sites are less than 1 km from the old company and these results
398 might indicate serious contamination due to the particulate material in this region. These data suggest a potential
399 concern in the area, and more detailed assessments of risks to human health are needed.
400 Median bioaccessible fractions (BAF) in the tailing samples were Pb (90%) > Cd (87%) > Zn (78%) >
401 Mn (63%) > Cu (61%), in soils: Cd (77%) > Pb (73%) > Mn (69%) > Zn (55%) > Cu (47%) and in sediments: Pb
402 (86%) > Mn (84%) > Cd (79%) > Zn (71%) > Cu (56%) (Figure 3). As for Pelfrêne et al (2017), respiratory
403 bioaccessibility was influenced by the composition of the matrices, such as oxides, carbonates, aluminate,
404 phosphate and silicate, as well as the chemical behaviour of each element and its ability to form soluble complexes

405 with ALF components. The high % bioaccessibility (> 50%) was observed for all elements in the most of samples
406 (Figure 3). This was expected, since the ALF is an aggressive solution because of its low pH (4,5) and the presence
407 of chelating agent able to dissolve some PHE components.). Pelfrêne et al. (2017) observed that the bioaccessibility
408 of the elements was higher using the ALF compared to the other simulated fluids and concluded that ALF solution
409 could be used to assess the lung bioaccessibility of PHE because it provides a more conservative estimation of the
410 bioaccessible PHE.

411 The Kruskal-Wallis non-parametric test ($p > 0.05$) was conducted to evaluate the differences in PHE
412 respiratory bioaccessibility according to the matrices. The BAF medians did not differ between all three matrices,
413 except for Mn, ($H(2) = 7.482$, $p = 0.024$), in which the sediment group differed from the soil and tailings matrices.
414 This is likely to be related to mineralogy of sediment samples, where there is predominance of 2:1 mineral (Figure
415 2). These samples had similar mineralogical composition in the clay fraction (Figure 2b). XRD analysis identified
416 the phyllosilicates minerals in the four samples, with Mica group minerals (ex., Illite (Il)), Smectites group
417 minerals (Sm), both are 2:1 mineral, and Kaolinite (Kt), which is 1:1 mineral.
418

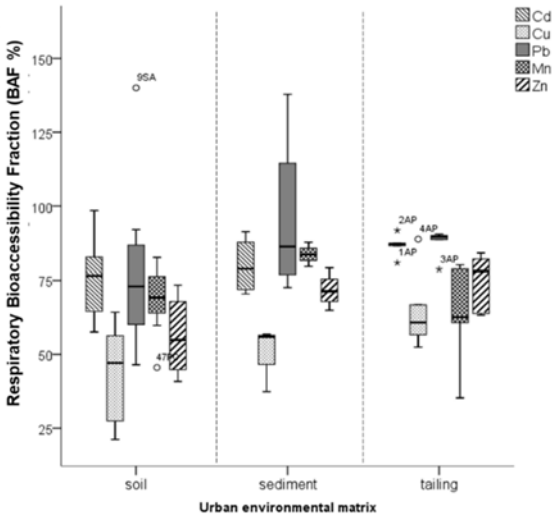

419

420 **Figure 3.** Box and whisker plot of the respiratory bioaccessible fraction (BAF %) of Cd, Cu, Mn, Pb and Zn
421 separated by type of matrix (Sediments (n = 4). Soil (n = 8) and Tailings (n = 5)). Asterisks are mean extremes,
422 and degree signs are outliers.
423

424 These results might imply that mineral phase controls the Mn bioaccessibility because the 2:1 clay
425 minerals have a large surface area and high cation exchange capacity, thus allowing high PHE sorption (Lamb et
426 al., 2009). Besides that, Mn is present in soils and sediments mainly in the form of oxides and hydroxides and can

427 be easily solubilized and incorporated into weathering products from soils (Gilkes and McKenzie, 1988). Other
428 factors may affect the dynamic of Mn on ALF fluids, such as pH and redox reaction that occurs in the matrix
429 (Hedberg et al., 2011). Similar Mn bioaccessibility (89%) was found by Hernández-Pellón et al. (2018) in PM_{10}
430 from a urban-industrial site in the north of Spain using ALF fluid. One of the ALF components is the citric acid
431 (20.8 g L^{-1}) which is able to reduce Mn (IV) to Mn (II) and make it soluble. The citric acid is a tricarboxylic organic
432 acid that promotes the dissolution of Mn oxides, mainly amorphous oxides (Hedberg and Odnevall Wallinder,
433 2016) and is able to dissolve secondary minerals, such as kaolinite and 2:1 minerals (Ramos et al., 2011), because
434 of the high metal complexation capacity of the carboxyl group.

435 Mn is one of the elements not included in the table of background guideline values for Brazilian soils
436 (CONAMA, 2012), although it is essential for humans for the synthesis and metabolism of neurotransmitters
437 (Dieter et al., 2005). Prolonged exposure to fumes and dust containing high concentrations of Mn represents a risk
438 factor for diseases such as Parkinson's (Kwakye et al., 2015) or Alzheimer's (Tong et al., 2014), as well as diseases
439 associated with pulmonary inflammation (Santamaria and Sulsky, 2010). Studies on the contamination of soils or
440 dust by Mn and its effects on human health have not been considered so far in Brazil. According to the USEPA
441 (USEPA, 1995), the reference dose for Mn is 10 mg day^{-1} (or 0.14 mg kg^{-1} day^{-1} for 70 kg adults) for chronic
442 ingestion and the inhalation lowest-observed-adverse-effect level (LOAEL) is 0.793 mg m^{-3}. Neurotoxicity has
443 been reported in environments where there is chronic exposure containing > 1 mg m^{-3} of Mn (Santamaria and
444 Sulsky, 2010). As such, further studies focussed on Mn exposure are required, especially on the dose-effect
445 relationship (Santamaria and Sulsky, 2010).

446 Extraction with ALF fluid resulted in PHE proportions (BAF) equal to or greater than 100% in some
447 samples (Figure 3). This was probably because the ALF solution is a complex medium with a high concentration
448 of organic complexes, low pH (4.5) and is able to solubilize high concentrations of these elements (Pelfrêne et al.,
449 2017). Moreover, the high solid: solution ratio (1:1000) used in the procedure, unlike the solid: solution ratio in
450 the 3051A method (1:24), can contribute to a greater dissolution of the < 10 μm material (Guney et al., 2017).
451 Therefore, it is suggested that the pseudo-total concentration in these cases should be interpreted with caution for
452 risk assessment. The high release of bioaccessible PHE in the different matrices is due to the high complex forming
453 capacity of the solution that contains six types of organic chemical substances (0.077 g L^{-1} trisodium citrate
454 dihydrate, 0.059 g L^{-1} Glycine, 20.8 g L^{-1} Citric acid, 0.090 g L^{-1} disodium tartrate, 0.085 g L^{-1} sodium lactate and
455 0.172 g L^{-1} sodium pyruvate).

456 The release of PHE may increase with an increase in the capacity to form stable complexes and the
457 concentration of ligands in the solution (Hedberg et al., 2011). The effect of pH alone is not as significant as the
458 action of organic complexing agents and the number of available functional groups (Hedberg et al., 2011). The
459 presence of citric acid and other organic substances in the ALF fluid promotes the formation of complexes with
460 the metals, resulting in increased solubility, thus replacing the adsorbed metals on the surface of the particulate
461 matter and forming organometallic complexes in the ALF solution (Henderson et al., 2014; Kim et al., 2013).
462

463 **3.3 Influence of solid phase matrices in the respiratory bioaccessibility of potentially harmful elements**

464 *3.3.1 Sequential extraction*

465 A high variability of the geochemical phases in the soil, sediment and tailing matrices was observed in
466 the sequential extraction (BCR) results for all elements studied (Fig. 4 and S4). In the tailing samples, the PHE
467 most associated with the F1, that is the mobile phase and bound to carbonates of the environmental matrices, were
468 Mn, Cd and Zn (median 30, 44 and 51%, respectively) compared to the other elements studied (Figure 4). High
469 concentrations of carbonates are generally found in environmental matrices with pH > 6 (Hooda, 2010). In this
470 case, the PHE would be associated or precipitated with carbonated minerals that may be dissolved by 0.11 M
471 CH_3COOH solution. For example, Khanmirzaei et al. (2013) observed that the HCO_3^- anion was the main Cd
472 complexing in the soil solution (slightly alkaline pH values), and that the dominant species in solution were Cd^{2+}
473 and $CdHCO^+_3$, deducing that $CdCO_3$ can control Cd^{2+} concentration in solution.
474

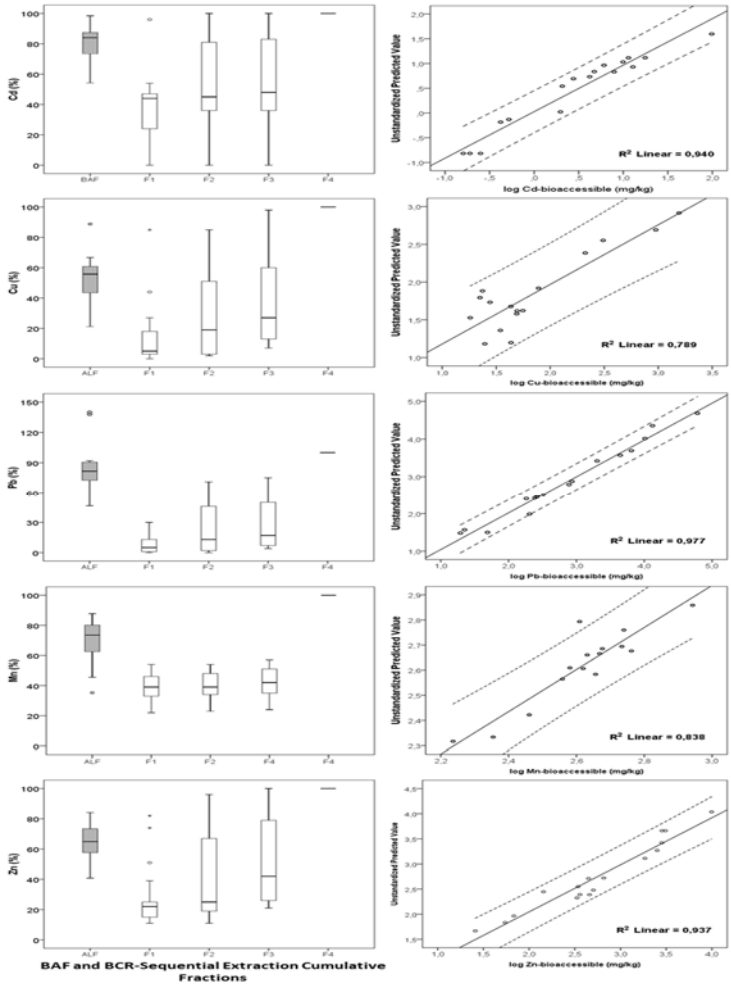

475

476 **Figure 4.** Cumulative solid-phase distribution and bioaccessible fraction (%) of potentially harmful elements in
477 samples of urban matrices (10 μm). BAF— bioaccessible fraction (%). F1: Exchangeable and acid soluble
478 carbonate fraction; F2: hydroxides and mixed oxy-hydroxide phases (reducible fraction); F3: Organic substance
479 and sulphide fraction (oxidizable fraction) and; F4: the residual non-silicate bound trace metal concentration (Left
480 side). Scatterplots of bioaccessible concentration (mg kg $^{-1}$) versus bioaccessible concentrations predicted by the
481 regression model (Right side).

482

483 Samples from Apiaí (1AP, 2AP, 3AP and 4AP) had Zn concentrations in F1 ranging from 39 to 84%
484 (2,830 to 9,920 mg kg^{-1}) of the pseudo-total concentration resulting in the accumulation of Zn in the surface of
485 matrix. The relative abundance of Zn in the solid fractions in tailing samples decreased in the order of F1 > F4 >
486 F2 > F3. These results were similar with those found by Kasemodel et al. (2019) in soil samples from a former Pb
487 slag deposit and in a Pb beneficiation Plant at Adrianópolis, state of Paraná, southern of Brazil.

488 In the sediment samples, 43 and 48% of Cd and Mn (median values), respectively are associated with the
489 F1. The F1 fraction of Cd varied from 0 to 49% in the soil samples, 23 to 84% in the tailing matrix, and 38 to 48%

490 in sediments. In soils, a higher proportion of Mn was found in F1 (median = 40%), though a soil sample (58PC)
491 had almost 85% of the total content in the F1 (Figure 4G). Hernández-Pellón et al. (2019) observed that Mn
492 compounds in the water-soluble fraction were highest than the other fractions in PM_{10} samples from an urban area
493 impacted by a Mn alloy plant. This may be because of Mn oxide reaction with NO_2, SO_2 and HCl gases from
494 atmosphere pollution found in industrial areas, producing soluble salts, i.e., $MnSO_4$, $Mn(NO_3)_2$, $Mn(NO_3)_2$, $MnCl_2$.
495 The water-soluble fraction is assumed to be part of F1 in the BCR-sequential extraction.

496 Three soil samples, two collected in the city of Piracicaba (35PC and 47PC), and one collected in a native
497 forest in the city of Apiaí (5AP) had the concentration of Cd extracted by the 0.11 mol L^{-1} acetic acid (Rauret et
498 al., 1999) lower than the LQ (0.005 mg L^{-1}). However, Cd was associated with either the F2, reducible fraction
499 (47PC = 99% and 5AP = 83%) or the F4, residual fraction (35PC = 100%). Colzato et al. (2017) observed similar
500 result in a Brazilian Typic Argiudoll which had 75% of Cd extracted by 0.5 mol L^{-1} $NH_2OH.HCl$.

501 A larger proportion of Pb and Cu (n = 17, median = 5%, percentile 25^{th}: 1.2 and 2.5 %; percentile 75^{th}:
502 13.4 and 18.7 %, respectively) were present in F1 compared to the other elements (Figure 4 C and E). This is most
503 likely to be due to a pH > 6 that favoured the formation of precipitates or insoluble substances and to the presence
504 of organic matter, since organic carbon ranged from 0.5 to 6.5% (Table 2), thus forming stable complexes with
505 PHE. Conversely, Witt III et al. (2014) evaluated Pb dust collected in a mining area and observed that the high
506 proportion of Pb in the mobile fraction was associated with the presence of cerussite ($PbCO_3$), litharge (PbO) and
507 anglesite ($PbSO_4$) that are soluble in acetic acid solution. However, in this study, the highest proportion of Pb was
508 found in F4 (residual) with median 89% for sediment, 86% for soils and 51% for tailing. In general, soil Pb is
509 immobile at high pH and when associated with silicate fraction (Shotyk and Le Roux, 2005).

510 In the F2 fraction (reducible phase) the behaviour of the elements is site-specific, i.e. soil samples 47PC,
511 5AP and 9SA showed Cd, Cu, Pb, Mn and Zn associated with this fraction, but this was not shown in the other
512 samples. The same behaviour was also observed in sediment 8SA and tailings samples 2AP, 3AP and 4AP. Tailing
513 samples had higher concentrations of Cd, Cu, Pb and Mn in F2 compared to the sediment and soil samples,
514 indicating that these elements may be bound to Fe/Mn oxides. A high median content was observed for Cu and Pb
515 (> 30%) in tailing samples 2AP, 3AP and 4AP, compared to Cd, Mn and Zn. Samples 1AP and 1SA did not have
516 levels available in this fraction (Figure S4).

517 In the samples not mentioned here Cd, Cu, Pb and Mn concentrations were below the limit of
518 quantification (0.01 mg L^{-1}) and some samples of sediments and soils had low concentrations of Zn on F2 (< 2 mg
519 kg^{-1}). Generally, soils from humid tropical regions have a high degree of weathering, predominating minerals such

520 as kaolinite and oxides/hydroxides of Fe and Al, such as hematite (Fe_2O_3), goethite (FeOOH) and gibbsite
521 ($Al(OH)_3$) whose electrical charge are highly pH dependent (Fontes and Alleoni, 2006). Therefore, extraction with
522 0.11 mol L^{-1} CH_3COOH (pH ≈ 2.9, pKa 4.76) may have formed positive charges by the adsorption of H^+ on the
523 edge surface causing the destabilization of the variable charges minerals releasing the metals to the extraction
524 solution (F1) thereby, the F2 may have been underestimated. Therefore, samples that may contain high content of
525 hematite or goethite were not fully solubilized, which prevented the release of oxide-occluded metals to solution.
526 The hydroxylamine hydrochloride reagent used in the F2 extraction can moderately dissolve Fe
527 oxides/hydroxides in soils or sediments; however Mn solubility is more significant, as shown by Chao (1972),
528 who evaluated the dissolution of Fe and Mn oxides in samples of soils and sediments with acidified hydroxylamine
529 hydrochloride. Chao (1972) observed that 50% of Mn and 1% of Fe from highly weathered soils were solubilized
530 and the major part of iron oxides remained in the residue. F3 is related to the oxidizable fraction of a test material,
531 that is, the fraction of the elements linked to organic matter or to sulphides (Rauret et al., 1999). There was little
532 expression of this fraction in all samples studied, with relative amounts < 17%.
533 The Kruskal-Wallis test showed that there were no differences in the distribution of Cu (H(2) = 5.809, *p*
534 = 0.055) and Mn (H(2); *p* = 0.277) values in the F3 and that for Cd (*p = 0.041*), Pb (*p = 0.020*) and Zn (*p = 0.002*)
535 there were differences in the distribution of data. The relative abundance of PHE in the different urban matrices
536 found in F3 decreases as follows: Cd in sediments (7%) > tailings (5%) > soils (1%), Cu in soil (12%) > sediment
537 (9%) > tailings (7%), Pb in soil (5%) ≈ sediment (4%) ≈ tailing (3%), Zn in soil (3%) ≈ sediment (3%) > tailing
538 (1%) and soil (12%) > sediment (9%) > tailing (6%)
539 When the two first fractions were examined together (sum of F1 (exchangeable and acid soluble
540 carbonate) + F2 (hydroxides and mixed oxy-hydroxide phases (reducible fraction))), the most mobilizable
541 elements were Cd (46%) and Mn (40%) in soils, Cd (43%) and Mn (50%) in sediments, and Zn (82%) > Cd (61%)
542 > Cu (54%) > Pb (45%) > Mn (40%) in tailings. The samples containing considerable proportions of PHE in the
543 mobile and reducible phases were likely to be derived from anthropogenic sources, while the less mobile
544 (oxidizable and residual) were linked to geogenic sources (Borgese et al., 2013; Patinha et al., 2015).
545 The soil samples were collected in urban regions of the Piracicaba city (Table 1) which is in one of the
546 main industrial centres of the interior region of the state of São Paulo. Cd, Cu and Zn are generally derived from
547 industries, vehicle traffic, exhaust fumes and atmospheric deposition (Shi et al., 2013) and can be found in
548 considerable proportions in urban soils. On the other hand, sediment and soil samples collected in Santo Amaro

549 (Table 1), which is a smaller and less industrialized city than Piracicaba, may have had the contribution of the
550 tailing used as streets paving, as well as domestic waste improperly deposited on the streets.

551 A high percentage of all elements (> 50%) are associated with residual fraction (F4) for all matrices, i.e.
552 these elements may be either related to the silicate matrix of the samples or present in several metal alloys not
553 dissolved by the reagent solutions used in the previous fractions. On the other hand, a low proportion of Cd was
554 found in samples 47PC (5%) with no significant amount in samples of soil (9SA) and tailings (3AP), as can be
555 seen in Figure S4 (Supplementary material); 2% of Cu in soil sample 58PC, 4% of Zn in sample 8SA (sediment)
556 and no significant amounts in the tailing samples 3AP and 4AP (Figure S4). These samples (with low Cd and Cu
557 amounts in the residual fraction) had the highest proportions of the PHE referenced, associated to F2, which could
558 be bound to the Mn oxides, but the pseudo-total concentration of Fe was higher than that of Mn (48 to 118 times)
559 suggesting that Fe may be controlling the mobility of the elements at this fraction.
560
561 *3.3.2 Identification of the sources of PHE bioaccessibility using BCR-sequential extraction and MLR*

562 When comparing results of the respiratory bioaccessibility extraction with the sequential extraction, it
563 was observed that the simulated fluid could extract all the solid phases in most of the samples (Figure S4),
564 including some of the residual phase. It means that it was able to extract those elements strongly adsorbed to the
565 crystalline phase of the matrix.

566 The chemical fractionation of urban environmental matrices provided the estimate of bioaccessibility of
567 Cd, Cu, Mn, Pb and Zn. The determination coefficients (R^2) ranged from 0.79 to 0.98 and in the SLF. The MLR
568 allowed identification of the main geochemical sources as significant predictors of the respiratory bioaccessibility.
569 The adjusted final models are shown in Table 3. The MLR presented both F1 (soluble and exchangeable phase)
570 and F3 (oxidizable fraction) as the main predictors for Cd bioaccessibility. Both fractions contributed with same
571 impact in the model (b_{F1} = 0.34 and b_{F3} = 0.32, R^2 = 0.94, $p < 0.001$). The ALF fluid (pH 4.5) dissolved Cd in all
572 solid fractions (Figures 4A and 4B) in the matrices; however, the impact of Cd bound to the
573 exchangeable/carbonate and oxidizable forms was stronger than the reducible and residual forms. Metals bound
574 to the exchangeable and carbonated phases can easily become mobile and available under low pH conditions, and
575 thereby potentially harmful to human health. Metals such Cd can produce reactive oxygen species (ROS) able to
576 cause inflammatory diseases in the lungs (Julien et al., 2011).
577

578 ***Table 3*** Model for prediction of respiratory bioaccessibility of Cd, Cu, Pb, Mn and Zn from urban environmental
579 matrices

Element	Equation model**	R^2	S.E.*
Cd	$logCd_{ALF} = 0.82 + 0.34\ logCd_{F1} + 0.32\ logCd_{F3}$	0.94	0.21
Cu	$logCu_{ALF} = 0.76 + 0.94\ log\ Cu_{F3}$	0.79	0.28
Pb	$logPb_{ALF} = 0.012 + 1.04\ logPb_{F4} + .082\ logPb_{F2}$	0.98	0.17
Mn	$logMn_{ALF} = - 0.53 + 1.03\ logMn_{F1} + 0.29\ logMn_{F4}$	0.84	0.07
Zn	$logZnALF = 0.87 + 0.81\ logZn_{F1}$	0.94	0.18

580 * Standard error of estimate

581 ** $p < 0.001$

582

583 The predicted model for Cu bioaccessibility (Figure 4D) only had F3 (the oxidizable fraction) as the main
584 factor that affected the bioaccessibility ($R^2 = 0.8$). This factor was already expected since Cu has high affinity to
585 organic complexes that can be associated with the oxidizable fraction (Yang et al., 2018). In the presence of
586 organic anions, Cd and Cu behaviours in the soil can be altered. The presence of acetate may increase the amount
587 of Cu associated with the organic matter, as well as in the presence of citrate, Cu linked to carbonate and occluded
588 in manganese oxides is less pronounced (Ahumada et al., 2001).

589 In the case of Pb, 98% of respiratory bioaccessibility can be explained by the covariates, F4 and F2 in
590 this model (Figure 4F). The impact of F4 (residual fraction) is greater than F2 (reducible), it can be verified by the
591 magnitude of the *t* statistic test ($t_{F4}(13) = 22.8$; $t_{F2}(13) = 5.2$). Pb bioaccessibility is highly dependent of
592 mineralogical composition and weathered conditions as well as to the phosphate present in the ALF fluid. The
593 presence of phosphate may limit the Pb solubility because of formation of low-soluble substances, such as
594 pyromorphite ($Pb_5Cl(PO_4)_3$), even in environments with low pH values (Schaider et al., 2007). In our study,
595 however, in which the bioaccessibility of Pb ranged from 46 to 140% of the pseudo-total content, it is possible
596 that there were Pb species with greater lability, such as halides and carbonates forms, Pb oxides or adsorbed on
597 surface of Fe and Mn hydroxide (Rieuwerts et al., 2000).

598 F1 (exchangeable/carbonates) and F4 (residual) were the predictive variables for Mn-bioaccessibility
599 with the fitted model explaining 80% of the variation (Figure 4H). The effect of F1 was higher than F4 ($t_{F1}(12) =$
600 1.0; $t_{F4}(12) = 0.3$). Mn bioaccessible varied from 35 to 88% and Mn-F1 varied from 22 to 54%. Similar

601 bioaccessibility fraction (52%) and labile fraction of Mn (71%) was found by (Voutsa and Samara, 2002) at urban
602 and industrial sites suggesting the predominance of soluble forms in urban atmospheric particles.
603 The MLR identified F1 as the only predictor of Zn bioaccessibility ($R^2 = 0.94$) (Figure 4J). The positive
604 correlation between Zn-ALF and Zn-F1 suggest that the Zn species are likely derived from poorly crystalline
605 secondary mineral forms easily soluble in soil solution (Molina et al., 2013). Molina et al. (2013) observed that
606 there was a higher Zn bioavailability and bioaccessibility in mine waste at pH 1.5 and 4.5 than at pH 7.4; and *in*
607 *vitro* bioaccessibility decreased as follows: mine waste > hydrozincite > hemimorphite > zincite ≈ smithsonite >>
608 sphalerite, where the first three materials contained more than 81% of Zn in the labile phase (exchangeable ions
609 and carbonates) and demonstrated that the mineralogy was the main factor that contributes to the bioaccessibility.
610
611 **4. Conclusions**
612 The Brazilian Resolution, CONAMA #420, recommends the use of strong acid solutions to extract
613 inorganic substances for soils sieved with a 2 mm mesh, but the use of these procedures to extract the contents of
614 PHE and the particle size do not necessarily estimate the respiratory bioaccessibility. Therefore, a more detailed
615 analysis from each contaminated site and adequate sample preparation is required. It is recommended that the
616 extraction be performed on particles with less than 10 μm to simulate the size fraction that can reach the respiratory
617 tract.
618 Mn bioaccessibility may have been influenced by mineralogy, especially in sediment samples, where
619 there was a predominance of 2: 1 minerals and kaolinite. Although Mn is not included in the Brazilian soil quality
620 guideline, the results of this study show that 35 to 88% of the pseudo-total Mn concentration is bioaccessible,
621 which suggests that this PHE requires further attention, mainly in a HHRA. In addition, the mine tailings samples
622 contained the highest pseudo-total concentrations of PHE in comparison to the soil and sediment samples, both in
623 the bulk soil and fine fraction. However, all three matrices contained more than 60% of bioaccessible PHE
624 contents. These results lead us to highlight the importance of including the *in vitro* method of respiratory
625 bioaccessibility to provide a more realistic estimate of PHE concentrations in UEM that are potentially available
626 to humans.
627 MRL models were useful to differentiate the main solid fractions that influence the PHE bioaccessibility,
628 and the variation in the respiratory bioaccessibility of PHE should be attributed to differences in both chemical
629 and mineralogical characteristics of the matrices.

More detailed investigation into contaminated areas can serve as a basis for determining the physicochemical characteristics of inhalable/respirable particulate materials, in addition to assessing possible adverse effects on the environment and human health.

This study may serve as a basis for toxicological studies and for the development of new strategies for evaluating sites considered contaminated. The different PHE do not necessarily have the same behaviour in different matrices. So, each case must be carefully investigated. The development of public policies by stakeholders should consider the bioaccessibility results as one of the evaluation criteria in the HHRA for each contaminated site, as well as the geochemical behaviour of each PHE so that there is adequate information to support a good estimate based on risk associated with the environmental matrix.

Acknowledgments

This study was supported by the São Paulo Research Foundation (FAPESP) [grants # 15/19332-9 and # 15/24483-9]; by the Brazilian National Council for Scientific and Technological Development (CNPq) [grant # 404164/2016]. The authors thank the Department of Geoscience, University of Aveiro, Portugal, for their support in the development of the laboratory work. Dr Marina Colzato at ESALQ is gratefully acknowledged for performing the ICP-OES analyses. The authors also acknowledge the assistance and support provided by the Centre for Research in Geochemistry and Geophysics of the Lithosphere (NUPEGEL-USP) in the mineralogical analyses.

CRediT authorship contribution statement

A.B.: Conceptualization, Investigation, Formal analysis, Data curation, Writing - Original Draft, Writing - review & editing and Funding acquisition. **C.P.:** Validation, Investigation, Resources and Writing - review & editing. **J.W.:** Conceptualization, Validation, Formal analysis and Writing - review & editing. **M.C.:** Formal analysis and Writing - review & editing. **L.A.:** Conceptualization, Resources, Supervision, Funding acquisition and Writing - review & editing

Conflict of Interest

The authors declare that they have no conflict of interest.

658 **References**

659 Abdu, N., Agbenin, J.O., Buerkert, A., 2012. Fractionation and mobility of cadmium and zinc in urban vegetable
660 gardens of Kano, Northern Nigeria. Environ. Monit. Assess. 184, 2057–2066.
661 https://doi.org/10.1007/s10661-011-2099-2
662 Ahumada, I., Mendoza, J., Escudero, P., Ascar, L., 2001. Effect of acetate, citrate, and lactate incorporation on
663 distribution of cadmium and copper chemical forms in soil. Commun. Soil Sci. Plant Anal. 32, 771–785.
664 https://doi.org/10.1081/CSS-100103908
665 Batista, A.H., Melo, V.F., Gilkes, R., Roberts, M., 2018. Identification of heavy metals in crystals of sand and silt
666 fractions of soils by scanning electron microscopy (SEM EDS/WD-EPMA). Rev. Bras. Cienc. do Solo
667 42. https://doi.org/10.1590/18069657rbcs20170174
668 Boisa, N., Elom, N., Dean, J.R., Deary, M.E., Bird, G., Entwistle, J.A., 2014. Development and application of an
669 inhalation bioaccessibility method (IBM) for lead in the PM10 size fraction of soil. Environ. Int. 70, 132–
670 142. https://doi.org/10.1016/j.envint.2014.05.021
671 Borgese, L., Federici, S., Zacco, A., Gianoncelli, A., Rizzo, L., Smith, D.R., Donna, F., Lucchini, R., Depero, L.E.,
672 Bontempi, E., 2013. Metal fractionation in soils and assessment of environmental contamination in
673 Vallecamonica, Italy. Environ. Sci. Pollut. Res. 20, 5067–5075. https://doi.org/10.1007/s11356-013-
674 1473-8
675 Calas, A., Uzu, G., Martins, J.M.F., Voisin, Di., Spadini, L., Lacroix, T., Jaffrezo, J.L., 2017. The importance of
676 simulated lung fluid (SLF) extractions for a more relevant evaluation of the oxidative potential of
677 particulate matter. Sci. Rep. 7. https://doi.org/10.1038/s41598-017-11979-3
678 Carvalho, F.M., 2013. Mapa do solo contaminado por elementos químicos em Santo Amaro da Purificação, in: I
679 Simpósio de Atualização Científica (SACSA). UFBA, Santo Amaro.
680 Cave, M., 2012. Bioaccessibility of potentially harmful soil elements. Environ. Sci. 21, 26–29.
681 CETEM – Centre for Mineral Technology, 2012. Santo Amaro (BA) coexists with socio-environmental liabilities
682 of former metallurgical industry. CETEM - Banco dados verbetes 4.
683 Chao, T.T., 1972. Selective Dissolution of Manganese Oxides from Soils and Sediments with Acidified
684 Hydroxylamine Hydrochloride. Soil Sci. Soc. Am. J. 36, 764–768.
685 https://doi.org/10.2136/sssaj1972.03615995003600050024x

686 Colombo, C., Monhemius, A.J., Plant, J.A., 2008. Platinum, palladium and rhodium release from vehicle exhaust
687 catalysts and road dust exposed to simulated lung fluids. Ecotoxicol. Environ. Saf. 71, 722–730.
688 https://doi.org/10.1016/j.ecoenv.2007.11.011
689 Colzato, M., Kamogawa, M.Y., Carvalho, H.W.P., Alleoni, L.R.F., Hesterberg, D., 2017. Temporal Changes in
690 Cadmium Speciation in Brazilian Soils Evaluated Using Cd L III -Edge XANES and Chemical
691 Fractionation. J. Environ. Qual. 46, 1206–1214. https://doi.org/10.2134/jeq2016.08.0316
692 CONAMA, – National Environment Council, 2012. RESOLUTION No. 420, December 28, 2009 Published in
693 Official Gazette 249 on 12/30/2009, pp. 81-84, in: Current Conama Resolutions Published between
694 September 1984 and January 2012. Ministry of the Environment (MMA), Brasília, DF, Brazil, pp. 748–
695 762.
696 Cruz, N., Rodrigues, S.M., Tavares, D., Monteiro, R.J.R.R., Carvalho, L., Trindade, T., Duarte, A.C., Pereira, E.,
697 Römkens, P.F.A.M.A.M., 2015. Testing single extraction methods and in vitro tests to assess the
698 geochemical reactivity and human bioaccessibility of silver in urban soils amended with silver
699 nanoparticles. Chemosphere 135, 304–311. https://doi.org/10.1016/j.chemosphere.2015.04.071
700 de Andrade Lima, L.R.P.P., Bernardez, L.A., 2011. Characterization of the lead smelter slag in Santo Amaro,
701 Bahia, Brazil. J. Hazard. Mater. 189, 692–699. https://doi.org/10.1016/j.jhazmat.2011.02.091
702 de Andrade, M.F., Moraes, L.R.S., 2013. Lead contamination in Santo Amaro defies decades of research and
703 delayed reaction on the part of the public authorities. Ambient. e Soc. 16, 63–80.
704 https://doi.org/10.1590/S1414-753X2013000200005
705 Dias, C.L., Lemos, M.M.G., Casarini, D.C.P., Ohba, M.S., de Oliveira Filha, M.T., 2006. Valores Orientadores de
706 intervenção e sua aplicação no gerenciamento de áreas contaminadas, in: XIV Congresso Brasileiro de
707 Águas Subterrâneas. Associação Brasileira de Águas Subterrâneas - ABAS, São Paulo, pp. 1–18.
708 Dieter, H.H., Bayer, T.A., Multhaup, G., 2005. Environmental copper and manganese in the pathophysiology of
709 neurologic diseases (Alzheimer's disease and manganism). Acta Hydrochim. Hydrobiol. 33, 72–78.
710 https://doi.org/10.1002/aheh.200400556
711 Dixon, J.., Weed, S.., 1989. Minerals in soil environments, 2sd ed. Soil Science Society of America, Madison,
712 Wisconsin, USA.
713 Donagema, G.K., Campos, D.V.B. de, Calderano, S.B., Teixeira, W.G., Viana, J.H.M., 2011. Manual de método
714 e análise de solo, 2nd ed. Embrapa Solos, Rio de Janeiro.

715 Drysdale, M., Ljung Bjorklund, K., Jamieson, H.E.H.E., Weinstein, P., Cook, A., Watkins, R.T., Bjorklund, K.L.,
716 Jamieson, H.E.H.E., Weinstein, P., Cook, A., Watkins, R.T., 2012. Evaluating the respiratory
717 bioaccessibility of nickel in soil through the use of a simulated lung fluid. Environ. Geochem. Health 34,
718 279–288. https://doi.org/10.1007/s10653-011-9435-x
719 FAO – Food and Agriculture Organization of the United Nations, 2014. World reference base for soil resources
720 2014. International soil classification system for naming soils and creating legends for soil maps, World
721 Soil Resources Reports No. 106.
722 Fontes, M.M.P.F., Alleoni, L.R.F.L., 2006. Electrochemical attributes and availability of nutrients, toxic elements,
723 and heavy metals in tropical soils. Sci. Agric. 63, 589–608. https://doi.org/10.1590/s0103-
724 90162006000600014
725 Galle, P., Berry, J.P., Galle, C., 1992. Role of alveolar macrophages in precipitation of mineral elements inhaled
726 as soluble aerosols. Environ. Health Perspect. 97, 145–147. https://doi.org/10.1289/ehp.9297145
727 Gilkes, R.J., McKenzie, R.M., 1988. Geochemistry and Mineralogy of Manganese in Soils, in: Manganese in Soils
728 and Plants. pp. 23–35. https://doi.org/10.1007/978-94-009-2817-6_3
729 Guney, M., Bourges, C.M.-J.M.J., Chapuis, R.P., Zagury, G.J., 2017. Lung bioaccessibility of As, Cu, Fe, Mn, Ni,
730 Pb, and Zn in fine fraction (< 20 μm) from contaminated soils and mine tailings. Sci. Total Environ. 579,
731 378–386. https://doi.org/10.1016/j.scitotenv.2016.11.086
732 Hedberg, Y., Hedberg, J., Liu, Y., Wallinder, I.O., 2011. Complexation- and ligand-induced metal release from
733 316L particles: Importance of particle size and crystallographic structure. BioMetals 24, 1099–1114.
734 https://doi.org/10.1007/s10534-011-9469-7
735 Hedberg, Y.S., Odnevall Wallinder, I., 2016. Metal release from stainless steel in biological environments: A
736 review. Biointerphases 11, 018901. https://doi.org/10.1116/1.4934628
737 Henderson, R.G., Verougstraete, V., Anderson, K., Arbildua, J.J., Brock, T.O., Brouwers, T., Cappellini, D.,
738 Delbeke, K., Herting, G., Hixon, G., Odnevall Wallinder, I., Rodriguez, P.H., Van Assche, F., Wilrich,
739 P., Oller, A.R., 2014. Inter-laboratory validation of bioaccessibility testing for metals. Regul. Toxicol.
740 Pharmacol. 70, 170–181. https://doi.org/10.1016/j.yrtph.2014.06.021
741 Hernández-Pellón, A., Mazón, P., Fernández-Olmo, I., 2019. Quantification of manganese species in particulate
742 matter collected in an urban area nearby a manganese alloy plant. Atmos. Environ. 205, 46–51.
743 https://doi.org/10.1016/j.atmosenv.2019.02.040

744 Hernández-Pellón, A., Nischkauer, W., Limbeck, A., Fernández-Olmo, I., 2018. Metal(loid) bioaccessibility and
745 inhalation risk assessment: A comparison between an urban and an industrial area. Environ. Res. 165,
746 140–149. https://doi.org/10.1016/j.envres.2018.04.014
747 Hooda, P.S., 2010. Trace Elements in Soils. Wiley. https://doi.org/10.1002/9781444319477
748 Huang, M., Chen, X., Zhao, Y., Yu Chan, C., Wang, W., Wang, X., Wong, M.H., 2014. Arsenic speciation in total
749 contents and bioaccessible fractions in atmospheric particles related to human intakes. Environ. Pollut.
750 188, 37–44. https://doi.org/10.1016/j.envpol.2014.01.001
751 Julien, C., Esperanza, P., Bruno, M., Alleman, L.Y., 2011. Development of an in vitro method to estimate lung
752 bioaccessibility of metals from atmospheric particles. J. Environ. Monit. 13, 621.
753 https://doi.org/10.1039/c0em00439a
754 Kasemodel, M.C., Papa, T.B.R., Sígolo, J.B., Rodrigues, V.G.S., 2019. Assessment of the mobility,
755 bioaccessibility, and ecological risk of Pb and Zn on a dirt road located in a former mining area—Ribeira
756 Valley—Brazil. Environ. Monit. Assess. 191, 1–15. https://doi.org/10.1007/s10661-019-7238-1
757 Kastury, F., Smith, E., Juhasz, A.L., 2017. A critical review of approaches and limitations of inhalation
758 bioavailability and bioaccessibility of metal(loid)s from ambient particulate matter or dust. Sci. Total
759 Environ. 574, 1054–1074. https://doi.org/10.1016/j.scitotenv.2016.09.056
760 Khanmirzaei, A., Bazargan, K., Amir Moezzi, A., Richards, B.K., Shahbazi, K., 2013. Single and sequential
761 extraction of cadmium in some highly calcareous soils of Southwestern Iran. J. Soil Sci. Plant Nutr. 13,
762 153–164. https://doi.org/10.4067/s0718-95162013005000014
763 Kim, J.O., Lee, Y.W., Chung, J., 2013. The role of organic acids in the mobilization of heavy metals from soil.
764 KSCE J. Civ. Eng. 17, 1596–1602. https://doi.org/10.1007/s12205-013-0323-z
765 Kreyling, W.G., 1992. Intracellular particle dissolution in alveolar macrophages. Environ. Health Perspect. 97,
766 121–126. https://doi.org/10.1289/ehp.9297121
767 Kwakye, G., Paoliello, M., Mukhopadhyay, S., Bowman, A., Aschner, M., 2015. Manganese-Induced
768 Parkinsonism and Parkinson's Disease: Shared and Distinguishable Features. Int. J. Environ. Res. Public
769 Health 12, 7519–7540. https://doi.org/10.3390/ijerph120707519
770 Lamb, D.T., Ming, H., Megharaj, M., Naidu, R., 2009. Heavy metal (Cu, Zn, Cd and Pb) partitioning and
771 bioaccessibility in uncontaminated and long-term contaminated soils. J. Hazard. Mater. 171, 1150–1158.
772 https://doi.org/10.1016/j.jhazmat.2009.06.124

773 Leelasakultum, K., Kim Oanh, N.T., 2017. Mapping exposure to particulate pollution during severe haze episode
774 using improved MODIS AOT-PM 10 regression model with synoptic meteorology classification.
775 GeoHealth 1, 165–179. https://doi.org/10.1002/2017gh000059
776 Lehnert, B.E., 1990. Alveolar Macrophages in a Particle "Overload" Condition. J. Aerosol Med. 3, S-9-S-30.
777 https://doi.org/10.1089/jam.1990.3.Suppl_1.S-9
778 Ljung, K., Siah, W.S., Devine, B., Maley, F., Wensinger, A., Cook, A., Smirk, M., 2011. Extracting dust from
779 soil: Improved efficiency of a previously published process. Sci. Total Environ. 410–411, 269–270.
780 https://doi.org/10.1016/j.scitotenv.2011.07.061
781 Ljung, K., Torin, A., Smirk, M., Maley, F., Cook, A., Weinstein, P., 2008. Extracting dust from soil: A simple
782 solution to a tricky task. Sci. Total Environ. 407, 589–593.
783 https://doi.org/10.1016/j.scitotenv.2008.09.007
784 Lu, Z.B., Kang, M., 2018. Risk assessment of toxic metals in marine sediments from the Arctic Ocean using a
785 modified BCR sequential extraction procedure. J. Environ. Sci. Heal. - Part A Toxic/Hazardous Subst.
786 Environ. Eng. 53, 278–293. https://doi.org/10.1080/10934529.2017.1397443
787 Luo, X.S., Yu, S., Li, X.D., 2011. Distribution, availability, and sources of trace metals in different particle size
788 fractions of urban soils in Hong Kong: Implications for assessing the risk to human health. Environ.
789 Pollut. 159, 1317–1326. https://doi.org/10.1016/j.envpol.2011.01.013
790 Marôco, J., 2011. Análise estatística com o SPSS Statistics, 5th ed. Pero Pinheiro, Lisbon.
791 Marques, M.R.C., Loebenberg, R., Almukainzi, M., 2011. Simulated biologic fluids with possible application in
792 dissolution testing. Dissolution Technol. 15–28. https://doi.org/10.1002/jps.23029
793 Martins, J., Figueiredo, B.R., 2014. Testes de mobilidade de chumbo e arsênio em solo contaminado em Apiaí
794 (SP). Geochim. Bras. 28, 189–200. https://doi.org/10.5327/Z0102-9800201400020007
795 Molina, R.M., Schaider, L.A., Donaghey, T.C., Shine, J.P., Brain, J.D., 2013. Mineralogy affects geoavailability,
796 bioaccessibility and bioavailability of zinc. Environ. Pollut. 182, 217–224.
797 https://doi.org/10.1016/j.envpol.2013.07.013
798 Moreda-Piñeiro, J., Moreda-Piñeiro, A., Romarís-Hortas, V., Moscoso-Pérez, C., López-Mahía, P., Muniategui-
799 Lorenzo, S., Bermejo-Barrera, P., Prada-Rodríguez, D., 2011. In-vivo and in-vitro testing to assess the
800 bioaccessibility and the bioavailability of arsenic, selenium and mercury species in food samples. TrAC
801 Trends Anal. Chem. 30, 324–345. https://doi.org/10.1016/j.trac.2010.09.008

802 Niu, J., Rasmussen, P.E., Hassan, N.M., Vincent, R., 2010. Concentration distribution and bioaccessibility of trace
803 elements in nano and fine urban airborne particulate matter: Influence of particle size. Water. Air. Soil
804 Pollut. 213, 211–225. https://doi.org/10.1007/s11270-010-0379-z
805 Oberdörster, G., Oberdörster, E., Oberdörster, J., 2005. Nanotoxicology: An Emerging Discipline Evolving from
806 Studies of Ultrafine Particles. Environ. Health Perspect. 113, 823–839. https://doi.org/10.1289/ehp.7339
807 Patinha, C., Durães, N., Sousa, P., Dias, A.C., Reis, A.P., Noack, Y., Ferreira da Silva, E., 2015. Assessment of
808 the influence of traffic-related particles in urban dust using sequential selective extraction and oral
809 bioaccessibility tests. Environ. Geochem. Health 37, 707–724. https://doi.org/10.1007/s10653-015-9713-
810 0
811 Pelfrêne, A., Cave, M.R., Wragg, J., Douay, F., 2017. In vitro investigations of human bioaccessibility from
812 reference materials using simulated lung fluids. Int. J. Environ. Res. Public Health 14, 112.
813 https://doi.org/10.3390/ijerph14020112
814 Puga, A.P., Melo, L.C.A., de Abreu, C.A., Coscione, A.R., Paz-Ferreiro, J., 2016. Leaching and fractionation of
815 heavy metals in mining soils amended with biochar. Soil Tillage Res. 164, 25–33.
816 https://doi.org/10.1016/j.still.2016.01.008
817 Ramos, M.E., Cappelli, C., Rozalén, M., Fiore, S., Huertas, F.J., 2011. Effect of lactate, glycine, and citrate on the
818 kinetics of montmorillonite dissolution. Am. Mineral. 96, 768–780.
819 https://doi.org/10.2138/am.2011.3694
820 Rauret, G., López-Sánchez, J.F., Sahuquillo, A., Rubio, R., Davidson, C., Ure, A., Quevauviller, P., 1999.
821 Improvement of the BCR three step sequential extraction procedure prior to the certification of new
822 sediment and soil reference materials. J. Environ. Monit. 1, 57–61. https://doi.org/10.1039/a807854h
823 Rieuwerts, J.S., Farago, M.E., Cikrt, M., Bencko, V., 2000. Differences in lead bioavailability between a smelting
824 and a mining area. Water. Air. Soil Pollut. 122, 203–229. https://doi.org/10.1023/A:1005251527946
825 Santamaria, A.B., Sulsky, S.I., 2010. Risk Assessment of an Essential Element: Manganese. J. Toxicol. Environ.
826 Heal. Part A 73, 128–155. https://doi.org/10.1080/15287390903337118
827 Schaider, L.A., Senn, D.B., Brabander, D.J., Mccarthy, K.D., Shine, J.P., 2007. Characterization of zinc, lead, and
828 cadmium in mine waste: Implications for transport, exposure, and bioavailability. Environ. Sci. Technol.
829 41, 4164–4171. https://doi.org/10.1021/es0626943
830 Shi, X., Chen, L., Wang, J., 2013. Multivariate analysis of heavy metal pollution in street dusts of Xianyang city,
831 NW China. Environ. Earth Sci. 69, 1973–1979. https://doi.org/10.1007/s12665-012-2032-1

832 Shotyk, W., Le Roux, G., 2005. Biogeochemistry and Cycling of Lead, in: Sigel, A., Siger, H., Siger, R.K. (Eds.),
833 Metal Ions in Biological Systems. CRC Press, pp. 239–275.
834 https://doi.org/10.1201/9780824751999.ch10
835 Tong, Y., Yang, H., Tian, X., Wang, H., Zhou, T., Zhang, S., Yu, J., Zhang, T., Fan, D., Guo, X., Tabira, T., Kong,
836 F., Chen, Z., Xiao, W., Chui, D., 2014. High Manganese, A Risk for Alzheimer's Disease: High
837 Manganese Induces Amyloid-β Related Cognitive Impairment. J. Alzheimer's Dis. 42, 865–878.
838 https://doi.org/10.3233/JAD-140534
839 Tronde, A., 2002. Pulmonary drug absorption: In vitro and in vivo investigations of drug absorption across the
840 lung barrier and its relation to drug physicochemical properties. Uppsala University.
841 Unda-Calvo, J., Martínez-Santos, M., Ruiz-Romera, E., 2017. Chemical and physiological metal bioaccessibility
842 assessment in surface bottom sediments from the Deba River urban catchment: Harmonization of PBET,
843 TCLP and BCR sequential extraction methods. Ecotoxicol. Environ. Saf. 138, 260–270.
844 https://doi.org/10.1016/j.ecoenv.2016.12.029
845 USEPA – United States Environmental Protection Agency, 2007. Method 3051A - Microwave assisted acid
846 digestion of sediments, sludges, soils, and oils (No. 3051A).
847 USEPA – United States Environmental Protection Agency, 1995. Integrated Risk Information System:
848 Manganese; CASRN 7439-96-5.
849 Voutsa, D., Samara, C., 2002. Labile and bioaccessible fractions of heavy metals in the airborne particulate matter
850 from urban and industrial areas. Atmos. Environ. 36, 3583–3590. https://doi.org/10.1016/S1352-
851 2310(02)00282-0
852 Wei, M., Chen, J., Sun, Z., Lv, C., Cai, W., 2015. Distribution of Heavy Metals in Different Size Fractions of
853 Agricultural Soils Closer to Mining Area and its Relationship to TOC and Eh, in: World Congress on
854 New Technologies. Barcelona, pp. 1–6.
855 WHO – World Health Organization, 2000. Air quality guidelines for Europe, 2nd ed. WHO Regional Office for
856 Europe, Copenhagen.
857 Wiseman, C.L.S., 2015. Analytical methods for assessing metal bioaccessibility in airborne particulate matter: A
858 scoping review. Anal. Chim. Acta 877, 9–18. https://doi.org/10.1016/j.aca.2015.01.024
859 Witt, E.C., Shi, H., Wronkiewicz, D.J., Pavlowsky, R.T., 2014. Phase partitioning and bioaccessibility of Pb in
860 suspended dust from unsurfaced roads in Missouri-A potential tool for determining mitigation response.
861 Atmos. Environ. 88, 90–98. https://doi.org/10.1016/j.atmosenv.2014.02.002

862 Wragg, J., Klinck, B., 2007. The bioaccessibility of lead from Welsh mine waste using a respiratory uptake test.
863 J. Environ. Sci. Heal. - Part A Toxic/Hazardous Subst. Environ. Eng. 42, 1223–1231.
864 https://doi.org/10.1080/10934520701436054
865 Yang, K., Zhang, T., Shao, Y., Tian, C., Cattle, S.R., Zhu, Y., Song, J., 2018. Fractionation, bioaccessibility, and
866 risk assessment of heavy metals in the soil of an urban recreational area amended with composted sewage
867 sludge. Int. J. Environ. Res. Public Health 15, 613. https://doi.org/10.3390/ijerph15040613
868 Zhao, S., Duan, Y., Lu, J.J., Gupta, R., Pudasainee, D., Liu, S., Liu, M., Lu, J.J., 2018. Chemical speciation and
869 leaching characteristics of hazardous trace elements in coal and fly ash from coal-fired power plants. Fuel
870 232, 463–469. https://doi.org/10.1016/j.fuel.2018.05.135
871 Zhong, L., Yu, Y., Lian, H. zhen, Hu, X., Fu, H., Chen, Y. jun, 2017. Solubility of nano-sized metal oxides
872 evaluated by using in vitro simulated lung and gastrointestinal fluids: implication for health risks. J.
873 Nanoparticle Res. 19, 1–10. https://doi.org/10.1007/s11051-017-4064-7

874 **Table 1.** Identification of urban environmental matrices, coordinates and sites characteristics of the local collection
875 of soil, sediments and tailing matrices
876 **Table 2.** Chemical and physical characterization, pseudo-total and bioaccessible concentrations of potentially
877 harmful elements (PHE) of samples collected in urban regions in Brazil
878 **Table 3.** Model for prediction of respiratory bioaccessibility of Cd, Cu, Pb, Mn and Zn from urban environmental
879 matrices
880
881 **Figure 1**. Distribution of potentially harmful elements in the bulk sample (2mm) and fine fraction (10μm) of the
882 urban environmental matrices. Data has been log-transformed for better visualization.
883 **Figure 2.** X-ray diffraction (XRD) of urban environmental matrices, indicating the presence of Kaolinite (Kt),
884 Gibbisite (Gb), Smectite mineral group (Sm), Illite (Il), Calcite (Ca), Vermiculite (Vm), Hydroxy-interlayered
885 Vermiculite (VHE), Lead oxide (Pb)
886 **Figure 5.** Box and whisker plot of the respiratory bioaccessible fraction (BAF %) of Cd, Cu, Mn, Pb and Zn
887 separated by type of matrix (Sediments (n = 4). Soil (n = 8) and Tailings (n = 5)). Asterisks are mean extremes,
888 and degree signs are outliers.
889 **Figure 4.** Cumulative solid-phase distribution and bioaccessible fraction (%) of potentially harmful elements in
890 samples of urban matrices (10 μm). BAF— bioaccessible fraction (%). F1: Exchangeable and acid soluble
891 carbonate fraction; F2: hydroxides and mixed oxy-hydroxide phases (reducible fraction); F3: Organic substance
892 and sulphide fraction (oxidizable fraction) and; F4: the residual non-silicate bound trace metal concentration (Left
893 side). Scatterplots of bioaccessible concentration (mg kg^{-1}) versus bioaccessible concentrations predicted by the
894 regression model (Right side).